



# Purpuroines A–J, halogenated alkaloids from the sponge *Iotrochota purpurea* with antibiotic activity and regulation of tyrosine kinases

Shi Shen<sup>a</sup>, Dong Liu<sup>a</sup>, Chen Wei<sup>a</sup>, Peter Proksch<sup>b</sup>, Wenhan Lin<sup>a,\*</sup>

<sup>a</sup> State Key Laboratory of Natural and Biomimetic Drugs, Peking University, Beijing 100191, PR China

<sup>b</sup> Institute of Pharmaceutical Biology and Biotechnology, Heinrich-Heine University, 40225 Duesseldorf, Germany

## ARTICLE INFO

### Article history:

Received 15 August 2012

Revised 15 October 2012

Accepted 17 October 2012

Available online 23 October 2012

### Keywords:

Marine sponge

*Iotrochota purpurea*

Purpuroines A–J

Structural elucidation

Kinase regulation

Antibiotic activity

## ABSTRACT

Ten new halogenated alkaloids named purpuroines A–J (**1–10**), and a known analogue (**11**), were isolated from the marine sponge *Iotrochota purpurea*. Their structures were elucidated by extensive spectroscopic (IR, MS, 1D and 2D NMR) data analyses. The inhibitory activity of some compounds against a panel of human disease related fungi and bacteria are evaluated. Bioassay for the regulation of tyrosine kinases revealed compounds **1** and **4** possessing selective inhibition against the kinase LCK. Primary structure–activity relationship is discussed.

© 2012 Elsevier Ltd. All rights reserved.

## 1. Introduction

Since the first halogenated secondary metabolite diiodotyrosine was isolated from the coral *Gorgonia cavolii*,<sup>1</sup> more than 300 bromotyrosine-derived natural products with a rich variety of chemical structures from marine organisms have been reported. These typical marine natural products are postulated to be generated via vanadium bromoperoxidases to incorporate bromine atom.<sup>2–4</sup> The chemo-ecological study revealed that the bromotyrosine-derived products exhibit chemical defense activity, such as the evidence that aerophobin-2 in the sponge *Aplysina aerophoba* is able to convert to verongiaquinol which contributes its cytotoxic activity against predators and to yield free radicals in the water surrounding the sponge to shield the sponge from predation or attack.<sup>5</sup> Consistent with the role as defensive effects, bromotyrosine-derived products exhibit a range of biological activities, including antitumor,<sup>6</sup> antiviral,<sup>7</sup> antifouling,<sup>8</sup> antifungal and antibacterial,<sup>9–11</sup> and anti-inflammatory effects.<sup>12</sup> Bromotyrosine-derived metabolites are even regarded as the chemical markers for taxonomic study of species in the order Verongida,<sup>13</sup> but this assumption is argued by the isolation of the related halogenated analogues from the sponge *Iotrochota birotulata* (order Poecilosclerida).<sup>14</sup> Our previous examination of *I. baculifera* also resulted in

the isolation of a diverse array of tyrosine-based alkaloids baculiferins, which showed potent Vif and APOBEC3G targeted anti-HIV activity.<sup>15</sup> In present work, a HPLC-ESIMS guiding fractionation of the sponge *I. purpurea* conducted to reveal the H<sub>2</sub>O soluble fraction containing diverse brominated components, which are never examined in previous work. Further chemical examination resulted in the isolation of eleven polyhalogenated alkaloids, which are evaluated for antibiotic and anti-kinase activities.

## 2. Results and discussion

### 2.1. Chemistry

Repeated column chromatography including Sephadex LH-20 and reversed-phase HPLC separation of *n*-BuOH soluble fraction from the EtOH extract of the sponge *I. purpurea* led to the isolation of 11 halogenated amino acids with trimethyl ammonium substituents (**1–11**) (Fig. 1), including a known analogue which was identified as *O*-methyl-*N*-trimethyl-3,5-dibromotyrosine (**11**).<sup>16</sup>

Purpuroine A (**1**) was obtained as a colorless amorphous. The ESIMS spectrum exhibited typical pseudomolecular ion peaks at *m/z* 472, 474, 476, 478 with the ratio of 1:3:3:1, containing three bromine atoms. Its molecular formula (C<sub>13</sub>H<sub>16</sub>Br<sub>3</sub>NO<sub>3</sub>) was determined by the HRESIMS data (*m/z* 471.8745 [M+H]<sup>+</sup>, Calcd 471.8759), requiring five degrees of unsaturation. The IR adsorption at 1680 cm<sup>−1</sup> in association with the <sup>13</sup>C NMR data at δ<sub>C</sub>

\* Corresponding author. Tel./fax: +86 10 82806188.

E-mail address: [whlin@bjmu.edu.cn](mailto:whlin@bjmu.edu.cn) (W. Lin).

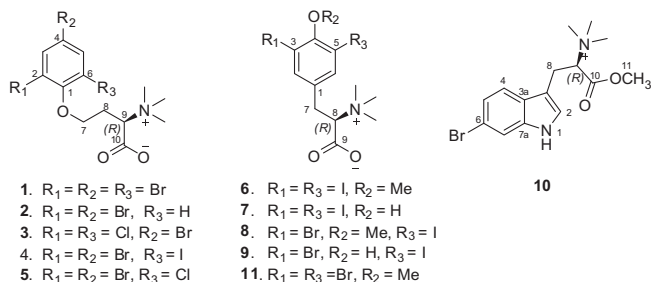


**Figure 1.** Structures of purpuroines A–J (**1**–**10**) and known analogue **11**.

166.9 suggested the presence of a carboxyl group. The  $^{13}\text{C}$  NMR and APT spectra (Table 2) disclosed a total of nine resonances, which were attributed to four aromatic carbons, a carbonyl carbon, two methylene carbons, a  $\text{sp}^3$  methine, and a methyl carbon. The COSY cross-peaks connected the alkyl signals to form a propane unit C<sub>7</sub>–C<sub>9</sub>, while HMQC relationship assigned the methylene C-7 ( $\delta_{\text{C}}$  72.0) to be oxygenated. The integration of a methyl singlet at  $\delta_{\text{H}}$  3.16 (s, 9H) in  $^1\text{H}$  NMR spectrum was characteristic of a trimethyl ammonium group,<sup>17</sup> while its position at C-9 was determined on the basis of the methyl protons correlated to C-9 ( $\delta_{\text{C}}$  74.8) in HMBC. Additional HMBC correlations from H<sub>2</sub>-8 ( $\delta_{\text{H}}$  2.20, 2.41, m) and H-9 ( $\delta_{\text{H}}$  3.58, dd,  $J = 2.3, 11.3$  Hz) to a carbonyl carbon at  $\delta_{\text{C}}$  166.9 in association with above NMR data disclosed a *N*-trimethylhomoserine. Moreover, two duplicated aromatic protons  $\delta_{\text{H}}$  7.95 (s, 2H) correlated to four aromatic carbons at  $\delta_{\text{C}}$  119.1 (C-2, C-6), 117.8 (C-4), 152.9 (C-1), and 135.5 (C-3, C-5) indicated a symmetrically substituted phenyl ring. Because the molecule contains three Br atoms, two possible substitutions involving a 2,4,6-tribrominated or 3,4,5-tribrominated phenyl ring are depicted. The absence of NOE interaction between aromatic protons and H<sub>2</sub>-7 ( $\delta_{\text{H}}$  4.12, 4.00) and the typical downfield shifted aromatic methines conducted to assign a 2,4,6-tribromophenyl unit. The connectivity of the phenyl ring to homoserine via ether bond across C-7 and C-1 was evident from the HMBC cross-peak between H<sub>2</sub>-7 and C-1. Because all *N*-trimethyl-*D*-homoserine derivatives such as nakirodin A<sup>17</sup> show positive sign of specific rotation, the positive sign at  $[\alpha]_{\text{D}}^{20} +10.8$  (c 0.24, MeOH) of **1** and the similar CD effects ( $\Delta\epsilon +0.11$  (215 nm),  $\Delta\epsilon -0.07$  (204 nm)) indicated the absolute configuration of C-9 to be *R*.

The molecular formula of purpuroine B (**2**) was determined as  $\text{C}_{13}\text{H}_{17}\text{Br}_2\text{NO}_3$  on the basis of the HRESIMS data ( $m/z$  415.9461  $[\text{M}+\text{Na}]^+$ , Calcd 415.9473), while the molecular ions at  $m/z$  416, 418, and 420 with the ratio of 1:2:1 confirmed two Br atoms in the molecule. Comparison of NMR data (Tables 1 and 2) ascertained that **2** is a 6-debrominated analogue of **1**. This assignment was confirmed by the presence of an aromatic ABX spin system at  $\delta_{\text{H}}$  7.81 (1H, d,  $J = 2.1$  Hz, H-3), 7.54 (1H, dd,  $J = 2.1, 8.7$  Hz, H-5), and 7.08 (1H, d,  $J = 8.7$  Hz, H-6) and the NOE interaction

between H-6 and H<sub>2</sub>-7 (4.17, t). The configuration of C-9 in **2** is the same as that of **1** due to the same sign of specific rotation and similar CD effects.

Purpuroine C (**3**) exhibited a cluster of pseudomolecular ion peaks at  $m/z$  406, 408, 410, 412  $[\text{M}+\text{Na}]^+$  with the ratio of 9:15:6:1 in ESIMS, requiring one Br and two Cl atoms in the molecule. The HRESIMS data ( $m/z$  405.9584  $[\text{M}+\text{Na}]^+$ , Calcd 405.9588) was in accordance with the molecular formula of  $\text{C}_{13}\text{H}_{16}\text{BrCl}_2\text{NO}_3$ . The NMR data of **3** indicated the presence of a *N*-trimethylhomoserine unit, and a symmetrically substituted phenyl ring due to the duplicated aromatic protons at  $\delta_{\text{H}}$  7.83 (s, 2H). The aromatic protons were assigned to H-3 and H-5 rather than H-2 and H-6 based on the absence of their NOE interactions with H<sub>2</sub>-7. The HMBC interaction between H<sub>2</sub>-7 and C-1 ( $\delta_{\text{C}}$  151.0) confirmed an ether bond connected C-1 and C-7. Thus, C-2 and C-6 were substituted by Cl atoms, whereas C-4 was positioned by Br atom.

The NMR spectroscopic data of purpuroine D (**4**) (Tables 1 and 2) indicated it shares a *N*-trimethylhomoserine unit of **1**, while the difference was attributed to the aromatic substitution. The ESIMS displayed pseudomolecular ions at  $m/z$  520, 522 and 524 with the ratio of 1:2:1 isotopic distribution, indicating the presence of two Br atoms. The HRESIMS ( $m/z$  519.8608, Calcd 519.8620) and NMR data established its molecular formula of  $\text{C}_{13}\text{H}_{16}\text{Br}_2\text{INO}_3$ . In  $^1\text{H}$  NMR spectrum, the *meta*-coupling aromatic protons at  $\delta_{\text{H}}$  7.95 (d,  $J = 2.1$  Hz, H-3) and 8.06 (d,  $J = 2.1$  Hz, H-5) disclosed an asymmetrical substitution in phenyl ring. An ether bond across C-7 and C-1 was determined by the HMBC correlation between H<sub>2</sub>-7 and C-1. The absence of NOE interaction between aromatic protons and H<sub>2</sub>-7 suggested the positions of the aromatic protons at H-3 and H-5. Thus, the halogen atoms are assumed to be as 2,4-dibromo-6-iodo substitution. The typical upfield of iodo-substituted carbon C-6 ( $\delta_{\text{C}}$  95.3) and the HMBC correlation between C-6 and H-5 without the correlation between H-3 and C-6 further supported the location of halogen atoms.

The NMR data of purpuroine E (**5**) are closely related to **4**, whereas its HRESIMS data ( $m/z$  427.9251  $[\text{M}+\text{H}]^+$ , Calcd 427.9264) provided the molecular formula ( $\text{C}_{13}\text{H}_{16}\text{Br}_2\text{ClNO}_3$ ) which contains a Cl atom instead of I atom of the latter compound. Analyses of 2D NMR revealed the structure of **5** differed from **4** due to the substituent at C-6 of **5** to be resided by a Cl atom. This assignment was evidenced by the chemical shift of C-6 ( $\delta_{\text{C}}$  129.7) appearing more downfield than that of **4**.

The absolute configuration of C-9 in **2**–**5** was determined as *R* on the basis of the same sign of specific rotation and similar CD effects as those of **1**.

The molecular formula of purpuroine F (**6**) was determined as  $\text{C}_{13}\text{H}_{17}\text{I}_2\text{NO}_3$  by HRESIMS ( $m/z$  489.9366  $[\text{M}+\text{H}]^+$ , Calcd 489.9376) and NMR data, indicating five degrees of unsaturation. The  $^1\text{H}$  and  $^{13}\text{C}$  NMR data (Tables 2 and 3) disclosed **6** to be a tyrosine derivative, closely related to the known analogs isolated from the sponge *Pseudoceratina crassa*.<sup>13</sup> The methyl singlet at  $\delta$  3.14 (9H,

**Table 1**  
 $^1\text{H}$  NMR data of **1**–**5** (DMSO- $d_6$ )

No.	<b>1</b>	<b>2</b>	<b>3</b>	<b>4</b>	<b>5</b>
3	7.95, s	7.81, d(2.1)	7.83, s	7.95, d(2.1)	7.93, d(2.2)
5	7.95, s	7.54, dd(8.7, 2.1)	7.83, s	8.06, d(2.1)	7.85, d(2.2)
6		7.08, d(8.7)			
7	4.12, dd(15.8, 8.4) 4.00, ddd(13.8, 8.7, 5.0)	4.17, m	4.14, m 4.04, ddd(13.6, 8.7, 4.9)	4.08, dd(15.2, 8.3) 3.96, ddd(14.2, 9.1, 5.4)	4.13, dd(16.2, 8.0) 4.02, ddd(13.5, 8.6, 5.0)
8	2.41, m 2.20, m	2.37, m 2.07, m	2.37, m 2.15, m	2.41, m 2.25, m	2.40, m 2.19, m
9	3.58, dd(11.3, 2.3)	3.55, br d(10.5)	3.57, dd(11.1, 2.4)	3.59, br d(10.3)	3.58, dd(11.3, 2.0)
N-(Me) <sub>3</sub>	3.16, s	3.16, s	3.15, s	3.17, s	3.16, s

**Table 2**  
<sup>13</sup>C NMR data of **1–9** (DMSO-*d*<sub>6</sub>)

No.	1	2	3	4	5	6	7	8	9
1	152.9	154.6	151.0	155.4	152.0	138.1	132.9	137.9	132.7
2	119.1	112.8	129.9	117.4	119.4	140.7	140.1	139.8	138.5
3	135.3	135.1	132.1	136.0	134.7	91.4	87.6	115.7	111.1
4	117.8	112.6	116.8	118.2	117.3	157.3	154.9	154.8	154.9
5	135.1	132.2	132.1	140.8	132.7	91.4	87.6	93.1	90.8
6	119.1	115.9	129.9	95.3	129.7	140.7	140.1	134.8	133.7
7	72.0	67.1	72.1	71.8	72.1	31.4	31.2	31.7	31.5
8	28.2	27.5	28.3	28.2	28.2	79.1	79.4	79.1	79.8
9	74.8	75.0	74.9	74.7	74.8	166.4	166.9	166.3	167.2
10	166.9	167.2	166.9	166.9	166.9				
N(Me) <sub>3</sub>	51.1	51.2	51.2	51.2	51.2	51.4 60.6	51.4	51.4 60.6	51.5

**Table 3**  
<sup>1</sup>H NMR data of **6–9**

Position	6	7	8	9
2	7.73, s	7.60, s	7.73, s	7.46, s
6	7.73, s	7.60, s	7.56, s	7.29, s
7	3.10, br d (12.1)	3.02, br d (11.5)	3.11, br d (12.1)	2.99, br d (11.1)
	2.89, t (12.1)	2.83, t (11.5)	2.92, t (12.1)	2.81, t (11.1)
8	3.61 br d (12.1)	3.60, br d (11.5)	3.62, br d (12.1)	3.58, br d (11.1)
N(Me) <sub>3</sub>	3.14, s	3.14, s	3.15, s	3.13, s
OMe	3.72, s		3.75, s	

s) as observed in **1–5** was attributed to a trimethyl ammonium unit, which was deduced to be positioned at C-8 on the basis of the HMBC correlation. The duplicated aromatic singlet at  $\delta$  7.73 (2H, s) was assigned to H-2 and H-6 according to their correlation with the methylene carbon C-7 ( $\delta$  31.4), indicating a symmetrical substitution in aromatic ring. A methoxy group was positioned at C-4 on the basis of the HMBC relationship between the methyl protons ( $\delta$  3.72, s) and C-4 ( $\delta$  157.3). Thus, positions C-3 and C-5 are substituted by iodine atoms.

The structure of purpuroine **G** (**7**) was determined as an analogue of **6** with OH-4 substitution based on the absence of methoxy group and the molecular formula (C<sub>12</sub>H<sub>15</sub>I<sub>2</sub>NO<sub>3</sub>) to be 14 amu less than that of **6**.

The NMR data (Tables 2 and 3) indicated the differences of purpuroine **H** (**8**) and **6** are in the substituents at aromatic ring. The molecular formula of **8** was determined as C<sub>13</sub>H<sub>17</sub>BrINO<sub>3</sub> on the basis of HRESIMS (*m/z* 441.9502 [M+H]<sup>+</sup>, Calcd 441.9515) and NMR data, containing a bromine and an iodine atom. The <sup>1</sup>H NMR spectrum exhibited two *meta*-coupled aromatic protons at  $\delta$  7.73 (br) and  $\delta$  7.56 (br), while their correlation with C-7 in HMBC conducted to assign the positions of the aromatic protons as H-2 and H-6. Additional HMBC interactions from the aromatic protons and methoxy protons to a carbon at  $\delta$  154.8 led to the assignment of methoxy group at C-4. Thus C-3 and C-5 must be substituted by Br and I atom, respectively.

The structure of purpuroine **I** (**9**) was determined to be OH-4 analog of **8** on the basis of NMR and MS data analyses.

The absolute configuration of C-8 in **6–9** was established as *R* by their positive specific rotation in contrast to the negative sign for **8S** of the authentic sample of *L*-N-trimethyl-3,5-dibromotyrosine.<sup>18</sup>

Purpuroine **J** (**10**) showed the pseudomolecular ion peaks at *m/z* 339 and 341 with a ratio of 1:1 in ESIMS, implying it contains one bromine atom. The molecular formula of **10** was established as C<sub>15</sub>H<sub>20</sub>BrN<sub>2</sub>O<sub>2</sub> by HRESIMS and NMR data. IR absorption at 1744 cm<sup>-1</sup> was attributed to carboxyl group. The <sup>1</sup>H and <sup>13</sup>C NMR spectra of **10** showed high similarity to those of 6-bromohypaphorine<sup>19</sup> except that the carboxylic group was replaced by methyl ester. Thus, the structure of **10** was determined as

**Table 4**  
Antimicrobial activities of compounds<sup>a</sup>

Compounds	IC <sub>50</sub> (μg/mL)		
	<i>S. pneumonia</i>	<i>C. albicans</i>	<i>A. fumigates</i>
<b>1</b>	NA	NA	28.58 ± 0.52
<b>3</b>	NA	NA	26.07 ± 0.55
<b>4</b>	NA	19.03 ± 0.12	25.56 ± 0.44
<b>9</b>	18.06 ± 0.76	NA	NA
Ampicillin	0.38 ± 0.029	NT	NT
Amphotericin B	NT	4.26 ± 0.14	3.27 ± 0.16

<sup>a</sup> Compounds **2**, **5–7**, **9** and **10** were inactive at concentration of 20 μg/ml; NA = no active; NT = no test.

6-bromohypaphorine methylate. Because the specific rotation of *D*-6-bromohypaphorine ( $[\alpha]_D^{19} -27^\circ$ )<sup>19</sup> and *L*-6-bromo hypaphorine ( $[\alpha]_D^{15} +58^\circ$ )<sup>20</sup> are reported, almost zero specific rotation of **10** suggested it to be a racemic mixture.

## 2.2. Bioactivity

### 2.2.1. Antibiotic activity

Compounds **1–4**, **7–9** and **11** representing halogenated homoserine and tyrosine-type derivatives are selected for antibiotic test against a panel of nine human disease related bacteria and fungi, including *Staphylococcus aureus*, *Streptococcus pneumonia*, *Escherichia coli*, *Pseudomonas aeruginosa*, *Candida albicans*, *Saccharomyces cerevisiae*, *Aspergillus fumigates*, *Aspergillus flavus*, and *Fusarium oxysporum*. The bioassay results (Table 4) revealed that homoserine derivatives **1** and **3** show selectively inhibition against fungus *A. fumigates*, which causes disease in individuals with an immunodeficiency. Compound **4** inhibited fungi *A. fumigates* and *C. albicans* selectively. However, the tyrosine-type derivative **9** exhibited selective inhibition against *S. pneumonia*, a significant human pathogenic and Gram-positive bacterium. The remaining compounds showed weak inhibition against the panel of microorganisms. The bioassay results indicated the halogen elements and their positions in aromatic ring directly affect the inhibitory activity.

**Table 5**  
Inhibitory activity against protein kinases

Compd	IC <sub>50</sub> (μg/mL)		
	LCK	CDK2	PLK1
<b>1</b>	2.35	>50	>50
<b>2</b>	12.76	>50	>50
<b>3</b>	4.52	>50	6.87
<b>4</b>	0.94	>50	1.45
<b>6</b>	7.17	>50	4.52
<b>7</b>	11.88	>50	10.06
<b>8</b>	7.91	>50	7.54
<b>9</b>	>50	>50	>50
<b>11</b>	>50	>50	>50
Staurosporine	3.73	11.76	0.92

### 2.2.2. Kinase inhibition

Kinase-targeted bioassay disclosed that **4** exhibited potent inhibition against LCK (lymphocyte-specific protein tyrosine kinase) (IC<sub>50</sub> = 0.94 μg/mL) and PLK1 (serine/threonine-protein kinase) (IC<sub>50</sub> = 1.45 μg/mL), while **1** showed selective inhibition against LCK (IC<sub>50</sub> = 2.35 μg/mL). Compounds **3**, **6**, and **8** showed moderate inhibition against LCK and PLK1 with IC<sub>50</sub> < 8.0 μg/mL. All compounds are weak inhibitors against CDK2 (cyclin-dependent kinase-2). Primary analyses of structure–activity relationship resulted in the trihalogen substituted analogues such as **1**, **3–4** possessing more inhibitory activity against LCK than dihalogenated analogue as **2** (Table 5), while homoserine-type analogues showed stronger inhibition against LCK than tyrosine-type derivatives. Kinase LCK plays a crucial role in T cell maturation and antigen-induced T cell activation. A LCK inhibitor possesses effectively block T cell function, acting as an immunosuppressive agent with potential therapeutic utility in treating autoimmune diseases.

## 3. Conclusion

Present work provides a new group of polyhalogenated alkaloids containing unique trimethyl ammonium group which is uncommonly found from nature. To the best of our knowledge, naturally occurring alkaloids with *N*-trimethylhomoserine are rarely reported. This finding provides additional evidence to argue the assumption that brominated tyrosine-derived metabolites are the chemical markers for taxonomic study of sponge species in the order Verongida.<sup>13</sup> Apart from the selective antibiotic activity, some compounds such as **1** and **4** selectively targeted on the tyrosine protein kinase LCK to induce its inhibition, suggesting they might be developed as a lead compounds of LCK inhibitors.

## 4. Experiments

### 4.1. Material and measurements

Optical rotations were measured on a Rudolph Research Analytical Autopol IV (Rudolph Research Co.). IR spectra were recorded on a Thermo Nicolet Nexus 470 FT-IR spectrometer. NMR spectra were measured on a Bruker Avance-500 FT 500 MHz NMR spectrometer using TMS as the internal standard. HRESIMS spectra were obtained on a LTQ Orbitrap XL Thermos Fisher Scientific. CD spectra were measured on a JASCO J-810 spectropolarimeter. Column chromatography was performed using silica gel (200–300 mesh, Merck). The GF<sub>254</sub> silica gel for TLC was provided by Sigma Co. Ltd Sephadex LH-20 (18–110 μm) was obtained from Pharmacia Co, and ODS (50 μm) was provided by YMC Co. High performance liquid chromatography (HPLC) was performed on an Alltech 426 apparatus with a 3300-ELSD UV detector. YMC HPLC column (C-8, 10 × 250 mm, S-5 μm, 12 nm) was used in the HPLC separation.

### 4.2. Marine sponge

Sponge *Iotrochota purpurea* was collected from the inner coral reef at a depth of around 10 m in Sanya Bay, Hainan Island of China, in 2009. The specimen was identified by Dr. Nicole J. de Voogd (National Museum of Natural History, The Netherlands). A voucher specimen (2009-S-1) was deposited at State Key Laboratory of Natural and Biomimetic Drugs, Peking University.

### 4.3. Extraction and isolation

The frozen sponge (10 kg) was homogenized and extracted with 70% EtOH–H<sub>2</sub>O (10 L × 3), and the EtOH solution was concentrated in vacuo to yield a residue (160 g). The residue was desalted by dissolving in MeOH and then filtrated. The concentrated MeOH extract was partitioned between H<sub>2</sub>O and EtOAc to remove lipids, and then H<sub>2</sub>O solution was extracted with *n*-BuOH. The concentrated *n*-BuOH fraction (7.0 g) was fractionated on ODS column eluting with a gradient MeOH–H<sub>2</sub>O (10–100%) to obtain five fractions (F1–F5). F3 and F4 were detected by HPLC–ESIMS to show the signals of halogen containing metabolites. F4 (1.2 g) was subjected to ODS column with a gradient MeOH–H<sub>2</sub>O (60–100%) to obtain **1** (80.2 mg), **2** (2.1 mg), **3** (1.6 mg), **5** (3.8 mg), **4** (2.1 mg), and **10** (3.8 mg). F3 (800 mg) was separated on Sephadex LH-20 column (70–100% MeOH–H<sub>2</sub>O) to obtain **9** (2.0 mg), **6** (3.8 mg), **7** (15.9 mg), **8** (5.8 mg), and **11** (46.6 mg).

#### 4.3.1. Purpuroine A (**1**)

Colorless amorphous;  $[\alpha]_D^{20}$  +10.8 (c 0.24, MeOH); UV(MeOH)  $\lambda_{\max}$  281, 289 nm; IR (KBr)  $\nu_{\max}$  1680, 1442, 1249, 1019 cm<sup>−1</sup>; CD (MeOH)  $\lambda_{\text{ext}}$  215 nm ( $\Delta\epsilon$  +0.11), 204 nm ( $\Delta\epsilon$  −0.07); <sup>1</sup>H and <sup>13</sup>C NMR data, see Tables 1 and 2; ESIMS *m/z* 472, 474, 476, 478 (1:3:3:1) [M+H]<sup>+</sup>; HRESIMS *m/z* 471.8745 [M+H]<sup>+</sup> (Calcd for C<sub>13</sub>H<sub>17</sub><sup>79</sup>Br<sub>3</sub>NO<sub>3</sub>, 471.8759).

#### 4.3.2. Purpuroine B (**2**)

Colorless oil;  $[\alpha]_D^{20}$  +27.1 (c 0.28, MeOH); UV(MeOH)  $\lambda_{\max}$  285 nm; IR (KBr)  $\nu_{\max}$  1689, 1468, 1286, 1049 cm<sup>−1</sup>; CD (MeOH)  $\lambda_{\text{ext}}$  225 nm ( $\Delta\epsilon$  +0.13), 203 nm ( $\Delta\epsilon$  −0.05); <sup>1</sup>H and <sup>13</sup>C NMR data, see Tables 1 and 2; ESIMS *m/z* 394, 396, 398 (1:2:1) [M+H]<sup>+</sup>; 416, 418, 420 (1:2:1) [M+Na]<sup>+</sup>; HRESIMS *m/z* 415.9461 [M+Na]<sup>+</sup> (Calcd for C<sub>13</sub>H<sub>17</sub><sup>79</sup>Br<sub>2</sub>NO<sub>3</sub>Na, 415.9473).

#### 4.3.3. Purpuroine C (**3**)

Colorless oil;  $[\alpha]_D^{20}$  +6.7 (c 0.18, MeOH); UV(MeOH)  $\lambda_{\max}$  283 nm; IR (KBr)  $\nu_{\max}$  1682, 1448, 1118, 1038 cm<sup>−1</sup>; CD (MeOH)  $\lambda_{\text{ext}}$  213 nm ( $\Delta\epsilon$  +0.10), 204 nm ( $\Delta\epsilon$  −0.06); <sup>1</sup>H and <sup>13</sup>C NMR data, see Tables 1 and 2; ESIMS *m/z* 406 (63), 408 (100), 410 (47), 412 (10) [M+Na]<sup>+</sup>; HRESIMS *m/z* 383.9766 [M+H]<sup>+</sup> (Calcd for C<sub>13</sub>H<sub>17</sub><sup>79</sup>Br<sup>35</sup>Cl<sub>2</sub>NO<sub>3</sub>, 383.9769).

#### 4.3.4. Purpuroine D (**4**)

Colorless oil;  $[\alpha]_D^{20}$  +4.1 (c 0.14, MeOH); UV(MeOH)  $\lambda_{\max}$  283, 292 nm; IR (KBr)  $\nu_{\max}$  1665, 1436, 1161, 1143, 1056 cm<sup>−1</sup>; CD (MeOH)  $\lambda_{\text{ext}}$  220 nm ( $\Delta\epsilon$  +0.12), 204 nm ( $\Delta\epsilon$  −0.04); <sup>1</sup>H and <sup>13</sup>C NMR data, see Tables 1 and 2; ESIMS *m/z* 520, 522, 524 (1:2:1) [M+H]<sup>+</sup>; 542, 544, 546 (1:2:1) [M+Na]<sup>+</sup>; HRESIMS *m/z* 519.8608 [M+H]<sup>+</sup> (Calcd for C<sub>13</sub>H<sub>17</sub><sup>79</sup>Br<sub>2</sub>INO<sub>3</sub>, 519.8620).

#### 4.3.5. Purpuroine E (**5**)

Colorless oil;  $[\alpha]_D^{20}$  +7.3 (c 0.16, MeOH); UV(MeOH)  $\lambda_{\max}$  281, 288 nm; IR (KBr)  $\nu_{\max}$  1698, 1446, 1383 cm<sup>−1</sup>; CD (MeOH)  $\lambda_{\text{ext}}$  214 nm ( $\Delta\epsilon$  +0.10), 204 nm ( $\Delta\epsilon$  −0.04); <sup>1</sup>H and <sup>13</sup>C NMR data, see Tables 1 and 2; ESIMS *m/z* 450 (53%), 452 (100%), 454 (75%), 456 (20%) [M+H]<sup>+</sup>; HRESIMS *m/z* 427.9251 [M+H]<sup>+</sup> (Calcd for C<sub>13</sub>H<sub>17</sub><sup>79</sup>Br<sub>2</sub><sup>35</sup>CINO<sub>3</sub>, 427.9264).



#### 4.3.6. Purpuroine F (6)

Colorless oil;  $[\alpha]_D^{20} +21.8$  (c 0.76, MeOH); IR (KBr)  $\nu_{\max}$  1668, 1461, 1415, 1385, 1114, 1034, 997  $\text{cm}^{-1}$ ;  $^1\text{H}$  and  $^{13}\text{C}$  NMR data, see Tables 2 and 3; HRESIMS  $m/z$  489.9366  $[\text{M}+\text{H}]^+$  (Calcd for  $\text{C}_{13}\text{H}_{18}\text{I}_2\text{NO}_3$ , 489.9376).

#### 4.3.7. Purpuroine G (7)

Colorless oil;  $[\alpha]_D^{20} +22.1$  (c 1.00, MeOH); IR (KBr)  $\nu_{\max}$  1668, 1463, 1385, 1118, 1049  $\text{cm}^{-1}$ ;  $^1\text{H}$  and  $^{13}\text{C}$  NMR data, see Tables 2 and 3; HRESIMS  $m/z$  475.9210  $[\text{M}+\text{H}]^+$  (Calcd for  $\text{C}_{12}\text{H}_{16}\text{I}_2\text{NO}_3$ , 475.9220).

#### 4.3.8. Purpuroine H (8)

Colorless oil;  $[\alpha]_D^{20} +31.5$  (c 1.16, MeOH); IR (KBr)  $\nu_{\max}$  1668, 1465, 1418, 1384, 1048  $\text{cm}^{-1}$ ;  $^1\text{H}$  and  $^{13}\text{C}$  NMR data, see Tables 2 and 3; ESIMS  $m/z$  442, 444 (1:1)  $[\text{M}+\text{H}]^+$ ; HRESIMS  $m/z$  441.9502  $[\text{M}+\text{H}]^+$  (Calcd for  $\text{C}_{13}\text{H}_{18}^{79}\text{BrINO}_3$ , 441.9515).

#### 4.3.9. Purpuroine I (9)

Colorless oil;  $[\alpha]_D^{20} +16.8$  (c 0.60, MeOH); IR (KBr)  $\nu_{\max}$  1669, 1468, 1078  $\text{cm}^{-1}$ ;  $^1\text{H}$  and  $^{13}\text{C}$  NMR data, see Tables 2 and 3; HRESIMS  $m/z$  427.9346, 429.9324 (1:1)  $[\text{M}+\text{H}]^+$  (Calcd for  $\text{C}_{12}\text{H}_{16}^{79}\text{BrINO}_3$ , 427.9358).

#### 4.3.10. Purpuroine J (10)

Colorless oil; IR (KBr)  $\nu_{\max}$  1743, 1682, 1445, 1207, 1137  $\text{cm}^{-1}$ ;  $^1\text{H}$  NMR ( $\text{DMSO}-d_6$ , 500 MHz)  $\delta$  11.27 (1H, s, NH), 7.57 (1H, d,  $J = 1.5$  Hz, H-7), 7.53 (1H, d,  $J = 8.6$  Hz, H-4), 7.23 (1H, d,  $J = 1.0$  Hz, H-2), 7.19 (1H, dd,  $J = 8.5$ , 1.5 Hz, H-5), 4.55 (1H, dd,  $J = 12.1$ , 2.5 Hz, H-9), 3.59 (1H, dd,  $J = 12.8$ , 2.5 Hz, H-8a), 3.33 (1H, dd,  $J = 12.1$ , 12.8 Hz, H-8b), 3.52 (3H, s, OMe), 3.17 (9H, s,  $\text{NCH}_3$ );  $^{13}\text{C}$  NMR ( $\text{DMSO}-d_6$ , 125 MHz)  $\delta$  167.8 (C-10), 137.6 (C-7a), 126.2 (C-2), 125.9 (C-3a), 122.1 (C-5), 120.5 (C-4), 114.8 (C-7), 114.7 (C-6), 74.1 (C-9), 53.5 (OMe), 49.5 ( $\text{NCH}_3$ ), 22.7 (C-8); HRESIMS  $m/z$  339.0700, 341.0679 (1:1)  $[\text{M}]^+$  (Calcd for  $\text{C}_{15}\text{H}_{20}\text{BrN}_2\text{O}_2$ , 339.0703).

#### 4.4. Antimicrobial assay

Antimicrobial bioassays were conducted in triplicate following the National Center for Clinical Laboratory Standards (NCCLS) recommendations.<sup>21</sup> Bacterial strains *Staphylococcus aureus*, *S. pneumoniae*, *Escherichia coli*, and *Pseudomonas aeruginosa* were grown on Mueller-Hinton agar. The yeasts *Candida albicans* and *Saccharomyces cerevisiae* were grown on Sabouraud dextrose agar, and the fungus *Aspergillus fumigatus* was grown on potato dextrose agar. Targeted microbes (3–4 colonies) were prepared from broth culture (bacteria: 37 °C for 24 h; fungus: 28 °C for 48 h), and the final spore suspensions of bacteria (in MHB medium), yeasts (in SDB medium), and fungus (in PDB medium) were 106 and 105 cells/mL and 104 mycelial fragments/mL, respectively. Testing compounds (10 mg/mL as stock solution in DMSO and serial dilutions) were transferred to a 96-well clear plate in triplicate, and the suspension of the test microorganisms were added to each well (200  $\mu\text{L}$ ) (antimicrobial peptide AMP, streptomycin, and fluconaz-

ole were used as positive controls). After incubation, the absorbance at 595 nm was measured with a microplate reader (TECAN), and the inhibition rate was calculated and plotted versus test concentrations.

#### 4.5. Kinase inhibition assay

The test for kinase inhibition was performed by the steps of kinase reaction, development reaction, and stop step, which are followed by the protocol in the literature.<sup>22,23</sup> The kinase inhibition was measured using a HTRF program under Beckman Coulter detector. Staurosporine is used as a positive control.

#### Acknowledgments

This work was supported by Grants from the NSFC (No.30930109), MOST 863 Project (2011AA090701, 2010DFA31610), and 2010319123366025-4.

#### Supplementary data

Supplementary data (the 1D and 2D NMR, IR, MS spectra) associated with this article can be found, in the online version, at <http://dx.doi.org/10.1016/j.bmc.2012.10.014>. These data include MOL files and InChIKeys of the most important compounds described in this article.

#### Reference and notes

- Dème, D.; Fimiani, E.; Pommier, J.; Nunez, J. *Eur. J. Biochem.* **1975**, *51*, 329.
- Vilter, H. *Phytochemistry* **1984**, *23*, 1387.
- Gribble, G. W. *Acc. Chem. Res.* **1998**, *31*, 141.
- Yamada, H.; Itoh, N.; Murakami, S.; Izumi, Y. *Agric. Biol. Chem.* **1985**, *49*, 2961.
- Koulman, A.; Proksch, P.; Ebel, R.; Beekman, A. C.; van Uden, W.; Konings, A. W.; Pedersen, J. A.; Pras, N.; Woerdenbag, H. J. *J. Nat. Prod.* **1996**, *59*, 591.
- Kreuter, M. H.; Bernd, A.; Holzmann, H.; Müller-Klieser, W.; Maidhof, A.; Weissmann, N.; Kljajic, Z.; Batel, R.; Schröder, H. C.; Müller, W. E. Z. *Naturforsch.* **1989**, *44c*, 680.
- Gunasekera, S. P.; Cross, S. S. *J. Nat. Prod.* **1992**, *55*, 509.
- Tsukamoto, S.; Kato, H.; Hirota, H.; Fusetani, N. *Tetrahedron* **1996**, *52*, 8181.
- Jang, J.; van Soest, R. W. M.; Fusetani, N.; Matsunaga, S. *J. Org. Chem.* **2007**, *72*, 1211.
- Fattorusso, E.; Minale, L.; Sodano, G. *J. Chem. Soc., Chem. Commun.* **1970**, 751.
- Fulmer, W.; van Lear, G. E.; Morton, G. O.; Mills, R. D. *Tetrahedron Lett.* **1970**, *11*, 4551.
- Gribble, G. W. *J. Chem. Educ.* **2004**, *81*, 1441.
- Ciminiello, P.; Fattorusso, E.; Magno, S.; Pansini, M. *J. Nat. Prod.* **1995**, *58*, 689.
- Costantino, V.; Fattorusso, E.; Mangoni, A.; Pansini, M. *J. Nat. Prod.* **1994**, *57*, 1552.
- Fan, G.; Li, Z.; Shen, S.; Zeng, Y.; Yang, Y.; Xu, M.; Bruhn, T.; Bruhn, H.; Morschhuser, J.; Bringmann, G.; Lin, W. *Bioorg. Med. Chem.* **2010**, *18*, 5466.
- Albrizio, S.; Ciminiello, P.; Fattorusso, E.; Magno, S.; Pansini, M. *Tetrahedron* **1994**, *50*, 783.
- Tsuda, M.; Endo, T.; Watanabe, K.; Fromont, J.; Kobayashi, J. *J. Nat. Prod.* **2002**, *65*, 1670.
- Gao, H.; Kelly, M.; Hamann, M. T. *Tetrahedron* **1999**, *55*, 9717.
- Kondo, K.; Nishi, J.; Ishibashi, M.; Kobayashi, J. *J. Nat. Prod.* **1994**, *57*, 1008.
- Raverty, W. D.; Thomson, R. H. *J. Chem. Soc., Perkin Trans. 1* **1977**, *10*, 1204.
- Li, E.; Jiang, L.; Guo, L.; Zhang, H.; Che, Y. *Bioorg. Med. Chem.* **2008**, *16*, 7894.
- Kleman-Leyer, K.; Lasky, D. A.; Klink, T. A. *Drug Discov. Devel.* **2003**, *6*, 81.
- Wang, M.; Wang, D.; Chen, Y. *Carcinogenesis* **2003**, *23*, 1291.